

# An illustrated anatomical ontology of the developing mouse lower urogenital tract

Kylie M. Georgas<sup>1</sup>, Jane Armstrong<sup>2</sup>, Janet R. Keast<sup>3</sup>, Christine E. Larkins<sup>4</sup>, Kirk M. McHugh<sup>5</sup>, E. Michelle Southard-Smith<sup>6</sup>, Martin J. Cohn<sup>4,7,8</sup>, Ekatherina Batourina<sup>9</sup>, Hanbin Dan<sup>9</sup>, Kerry Schneider<sup>9</sup>, Dennis P. Buehler<sup>6</sup>, Carrie B. Wiese<sup>6</sup>, Jane Brennan<sup>2</sup>, Jamie A. Davies<sup>2</sup>, Simon D. Harding<sup>10</sup>, Richard A. Baldock<sup>10</sup>, Melissa H. Little<sup>1,\*,#,§</sup>, Chad M. Vezina<sup>11,‡</sup> and Cathy Mendelsohn<sup>9,‡</sup>

## ABSTRACT

Malformation of the urogenital tract represents a considerable paediatric burden, with many defects affecting the lower urinary tract (LUT), genital tubercle and associated structures. Understanding the molecular basis of such defects frequently draws on murine models. However, human anatomical terms do not always superimpose on the mouse, and the lack of accurate and standardised nomenclature is hampering the utility of such animal models. We previously developed an anatomical ontology for the murine urogenital system. Here, we present a comprehensive update of this ontology pertaining to mouse LUT, genital tubercle and associated reproductive structures (E10.5 to adult). Ontology changes were based on recently published insights into the cellular and gross anatomy of these structures, and on new analyses of epithelial cell types present in the pelvic urethra and regions of the bladder. Ontology changes include new structures, tissue layers and cell types within the LUT, external genitalia and lower reproductive structures. Representative illustrations, detailed text descriptions and molecular markers that selectively label muscle, nerves/ganglia and epithelia of the lower urogenital system are also presented. The revised ontology will be an important tool for researchers studying urogenital development/malformation in mouse models and will improve our capacity to appropriately interpret these with respect to the human situation.

**KEY WORDS:** Mouse embryogenesis, Murine urogenital system development, Lower urinary tract, Lower reproductive tract, Urogenital sinus, Urethral plate, External genitalia, Genital tubercle, Bladder, Trigone, Ureter, Urethra, Pelvic urethra, Phallic urethra, Prostate gland, Pelvic ganglion

<sup>1</sup>Institute for Molecular Bioscience, The University of Queensland, St Lucia, Queensland 4072, Australia. <sup>2</sup>Center for Integrative Physiology, University of Edinburgh, Edinburgh EH8 9XD, UK. <sup>3</sup>Department of Anatomy and Neuroscience, University of Melbourne, Parkville, Victoria 3010, Australia. <sup>4</sup>Department of Molecular Genetics and Microbiology, University of Florida, Gainesville, FL 32610, USA. <sup>5</sup>Centre for Molecular and Human Genetics, The Research Institute at Nationwide Children's Hospital and Division of Anatomy, The Ohio State University, Columbus, OH 43205/10, USA. <sup>6</sup>Division of Genetic Medicine, Department of Medicine, Vanderbilt University School of Medicine, Nashville, TN 37232, USA. <sup>7</sup>Department of Biology, Genetics Institute, University of Florida, Gainesville, FL 32610, USA. <sup>8</sup>Howard Hughes Medical Institute, University of Florida, Gainesville, FL 32610, USA. <sup>9</sup>Columbia University, Department of Urology, New York, NY 10032, USA. <sup>10</sup>MRC Human Genetics Unit, MRC IGMM, Western General Hospital, Edinburgh EH4 2XU, UK. <sup>11</sup>University of Wisconsin-Madison, School of Veterinary Medicine, Madison, WI 53706, USA.

\*Present address: Murdoch Childrens Research Institute, Parkville, Victoria 3052, Australia.

<sup>‡</sup>These are equal last authors

<sup>§</sup>Author for correspondence (melissa.little@mcri.edu.au)

Received 2 November 2014; Accepted 1 April 2015

## INTRODUCTION

The urogenital tract is composed of urinary (kidneys, ureters, bladder, urethra) and reproductive (gonads, reproductive ducts, external genitalia) systems. The anatomy of this large, interconnected system is complex and changes rapidly during embryogenesis. In addition, hormonal signalling leads to dimorphism between male and female systems. With such complexity, even small perturbations in differentiation processes or timing in one tissue can translate into functional defects affecting the entire system. Congenital anomalies of the LUT have been described in both mouse models and humans (Rasouly and Lu, 2013). The embryonic origins and morphogenesis of the urogenital tract (bladder, urethra, vagina, external genitalia) and terminal hindgut (rectum and anus) are closely linked, which might explain the co-occurrence of genital anomalies (ambiguous genitalia, hypospadias, chordee and micropenis in males, cleft clitoris in females) with anorectal defects (Rasouly and Lu, 2013). Lower urinary and reproductive system development in mouse and human are not equivalent, and there have been historical instances in which terms have been drawn from human anatomy to incorrectly describe similar but distinct structures in the mouse. Clarity around the morphogenesis of these closely linked and intersecting organ systems in mouse will allow us to better appreciate differences between mouse and human, to re-evaluate the lessons that can or cannot be drawn from mouse models of human anomalies and, in some instances, to revise our thinking about the origin of some structures in the human.

Previously, we created a high-resolution anatomical ontology for the Genitourinary Development Molecular Anatomy Project (GUDMAP), a publicly available expression database for the mouse genitourinary system (Little et al., 2007). With the recent application of three-dimensional (3D) imaging techniques, the identification of cell-type specific markers and the application of genetic lineage tracing, our understanding of the developmental anatomy of the LUT and genitalia in the mouse have significantly improved. We have incorporated this new knowledge, together with additional studies presented here, into an updated anatomical ontology of the LUT and reproductive systems, including the sites and signalling centres important for establishing connections with the upper urogenital tract.

## RESULTS

### Early development: E10.5-14.5 (TS18-23)

Urogenital development involves epithelia derived from two embryological lineages, the nephric duct (ND, also called mesonephric or Wolffian duct) and cloaca, giving rise to the upper and lower urinary tract, respectively (reviewed in

supplementary material). At E11, the urogenital sinus (UGS) is a simple epithelial tube extending from the cloaca, to which paired NDs are attached via the common nephric duct (CND), defined as the region of ND caudal to the ureter (Fig. 1). Caudal NDs connect at the UGS ridge, a thickened, raised proportion of the UGS epithelium (Fig. 1A-C,I-M). The UGS ridge is a signalling centre, important for regulating CND remodelling and apoptosis during ureter maturation and repositioning (Shapiro et al., 2000). From E11-13, the anterior UGS above the UGS ridge is the primitive bladder, and below this site, including the UGS ridge itself, is the caudal UGS. We define the UGS region, in which the epithelia of the primitive bladder and caudal UGS meet, as the transition zone. The cranial UGS will elongate and expand, becoming the bladder, while the caudal UGS becomes the pelvic urethra (PLUR, Fig. 1).

The hindgut and anorectal sinus will form the colon, rectum and anus.

From E13, the term urethra is introduced, composed of pelvic and phallic regions. The PLUR develops within the embryo body and the phallic urethra (PHUR) within the GT (Fig. 1C,G,H). Alongside the NDs, paired paramesonephric ducts (derived from the mesonephric coelomic epithelium) elongate caudally and have reached the UGS ridge by E13.5 (Fig. 1C,M) (Guioli et al., 2007; Orvis and Behringer, 2007). From E14, the primitive bladder becomes the bladder. UGS is retained in the developmental ontology as a parental term, encompassing bladder, bladder-PLUR transition zone and PLUR.

The genital tubercle (GT) is the precursor of the penis and clitoris (supplementary material). Located within the GT of both sexes, the PHUR develops from a bilaminar epithelial extension of the cloacal

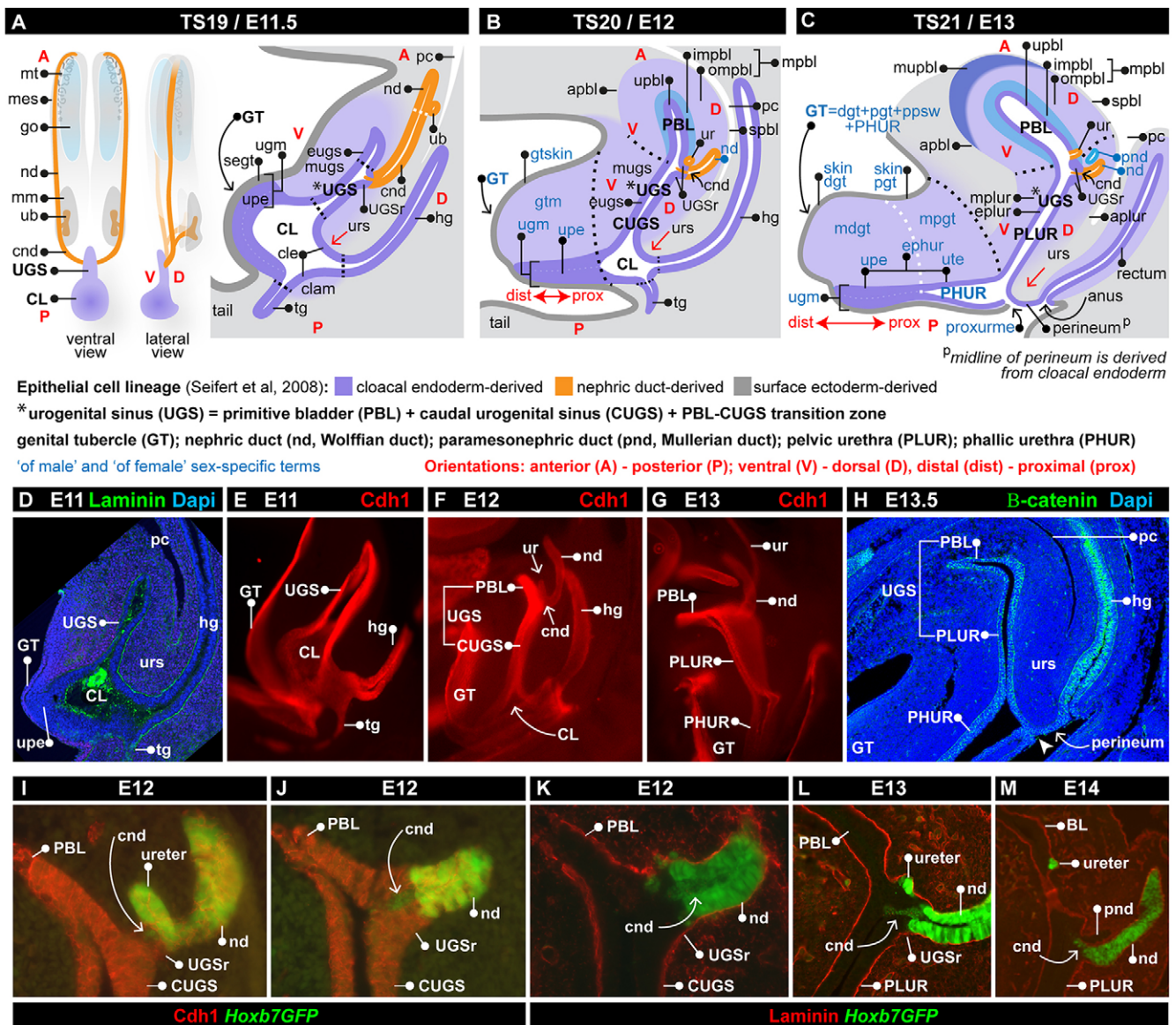


**Fig. 1. Urogenital sinus development.** (A-C) Schematics illustrating early development. (D-M) Immunohistochemistry of sagittal sections. Mesenchymal growth (red arrows, A-C) separates the hindgut and UGS. When it reaches the surface, the proximal urethral meatus is formed (C; arrowhead in H). Here, the perineum midline is derived from cloacal endoderm (C) and is  $\beta$ -catenin<sup>+</sup> (H). NDs connect the UGS ridge (A-C) and are Cdh1<sup>+</sup> (F,G). CND remodelling and ureter repositioning occur between E12 and E14 (B,C,I-M). NDs and CNDs are Hoxb7GFP<sup>+</sup> (I-M). UGS ridge is Cdh1<sup>+</sup> (I,J), Laminin<sup>+</sup> (K-M) and surrounds the CNDs at E11-12 (A,B,I,J). The ureter directly connects the bladder at E13 (C; Hoxb7GFP<sup>+</sup> in L). Very few Hoxb7<sup>+</sup> CND cells remain at E14 (M). For abbreviations in all Figures, see supplementary material.



epithelium, called the urethral plate epithelium (UPE). At the ventral midline, the endodermal cloacal epithelium is in direct contact with the surface ectoderm and together they are known as the cloacal membrane. By E11.5, genital swellings have merged to form a single GT, and the UPE grows out from between these swellings (Fig. 1A,D and Fig. 2A). As the urorectal septum expands, the UPE is forced into its ventral GT position and is in direct contact with the surface ectoderm/skin. Together, these structures are termed the urogenital membrane (Fig. 1A-C). At E13, the urorectal septum reaches the embryo surface, resulting in complete separation of the UGS and hindgut. Here, proportions of the cloacal membrane disintegrate in mice and humans, contributing to formation of the anal opening and an opening in the PHUR called the proximal urethral meatus (Fig. 1C,H and Fig. 2C; Nievelstein et al., 1998; Perriton et al., 2002; Sasaki et al., 2004; Seifert et al., 2008, 2009a,b; Lin et al., 2009; Ng et al., 2014; Ching et al., 2014; Miyagawa et al., 2014).

Except for very early in development (prior to E12), the GT and reproductive ducts are parts of the reproductive ontology. Whereas the PHUR in females plays no reproductive role, the term is included in both urinary and reproductive systems because of its anatomical location in the female external genitalia.

From E13, the GT is morphologically subdivided into proximal and distal regions (Fig. 1C and Fig. 2C). Laterally, in the proximal GT, two mesenchymal preputial swellings appear that enclose the preputial glands, epithelial glands seen from E13.5 (Cunha, 1975; Seifert et al., 2008). The PHUR epithelium remains in contact with the surface ectoderm of the ventral GT. The ventral ectoderm forms a small invagination, the urethral groove (or urethral seam), on the GT surface, where it meets the urethral endoderm (Baskin et al., 2001; Perriton et al., 2002). As seen in histological sections, the mouse urethra is actually closed within the GT, and therefore this groove has been referred to as a 'closed urethral groove' (Baskin

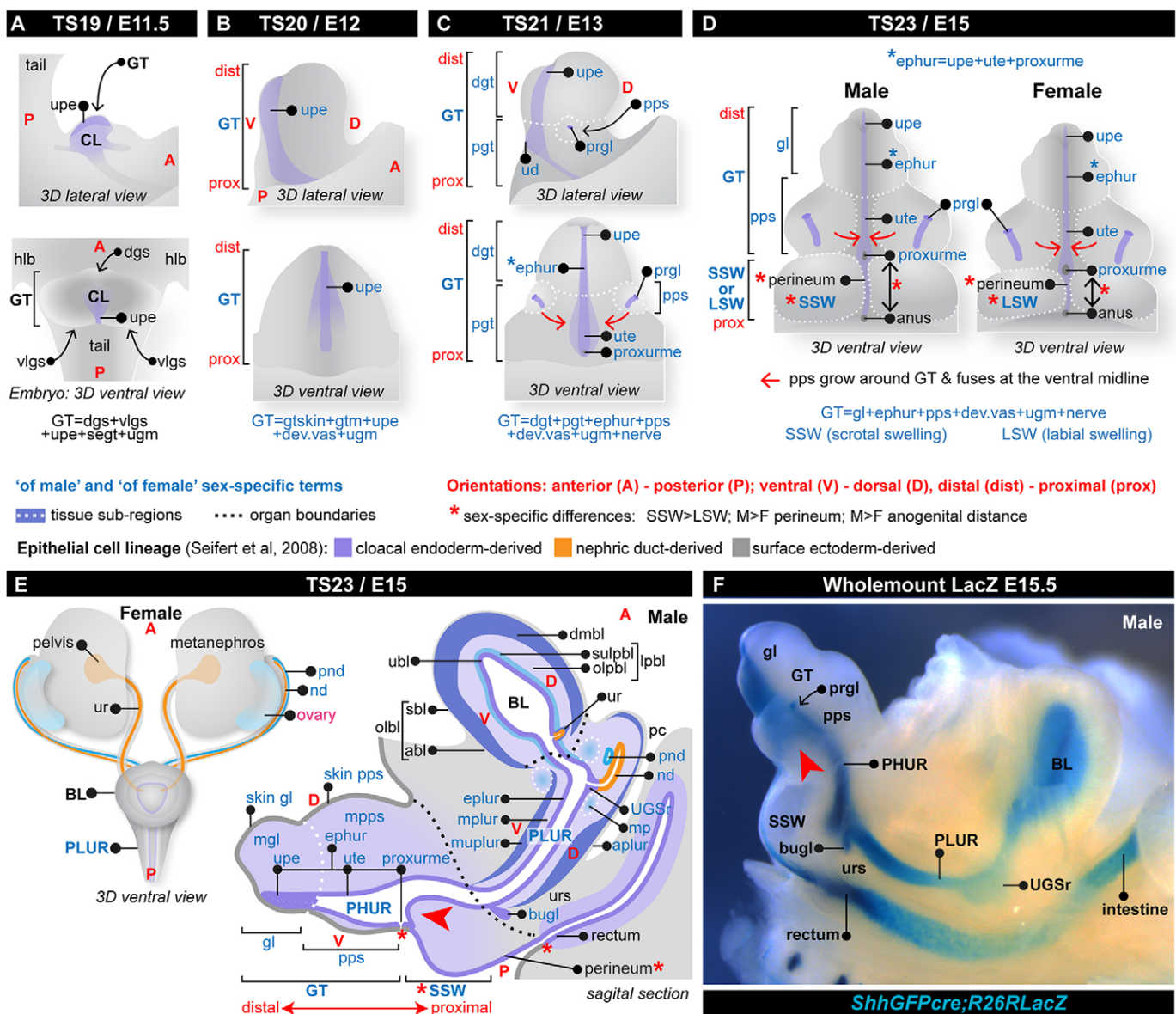


**Fig. 2. Genital tubercle development.** (A-E) Schematics illustrating GT development. Preputial swellings grow ventrally around the GT (red arrows). Anogenital distance, perineum and scrotal swellings are larger in males (red asterisks). (F) Whole-mount  $\beta$ -galactosidase staining of *ShhGFPcre;Rosa26RlacZ* embryo shows lineage of *Shh*-expressing cells (blue) in epithelia lining the PHUR, PLUR, bladder, rectum, intestine, perineum, bulbourethral glands, preputial glands and UGS ridge. In males, the mesenchyme begins to septate the PHUR epithelium (red arrowheads in E,F).

et al., 2001). This is in contrast to humans that develop an open urethral groove, with the PHUR lumen exposed on the ventral GT surface until fusion of the urethral folds results in closure (Glenister, 1954). The UPE commences as a cord that canalises in a proximal-to-distal wave, with the lumen forming between the two epithelial layers. From E13, the PHUR is composed of the distal UPE, proximal urethral tube epithelium and external orifice defined as the proximal urethral meatus (Fig. 1C and Fig. 2C). By E14 in both sexes, the preputial swellings become more apparent, and mesenchyme at the GT base expands and will become the labioscrotal swellings (Fig. 2D–F).

In histological section, mesenchymal swellings are found just lateral to the ventral-most urethral tube epithelium. This mesenchyme has been referred to as the ‘urethral folds’ (Yamada et al., 2003). We note that the ‘urethral folds’ described in the mouse are distinct from those structures of the same name in humans. Tubulogenesis of the human urethra is analogous to neurulation, in that the lateral edges of the urethral plate are brought together medially, eventually fusing to close the urethral tube. Fusion of the urethral folds in humans results in formation of the urethra proper internally and penile raphe externally, a structure that is not seen in the mouse. By contrast, the mouse UPE is a bilaminar epithelium that extends from the centre of the GT to the ventral margin, and lumen formation occurs as the two layers separate medially. In the mouse, the mesenchyme referred to as ‘urethral folds’ on either side of the plate might function to separate the definitive urethra from the ventral urethral seam, which will be remodelled away (Baskin et al., 2001).

### Sex-specific anatomical differentiation of LUT and external genitalia: E15.5 to adult (TS23–S28)

From E15, the GT is divisible proximo-distally into a proximal region surrounded by preputial swellings (and later, prepuce) and a distal region of exposed glans (Fig. 2D–F). During GT outgrowth (E11.5–14.5), males and females are anatomically indistinguishable. However, from E15.5, morphological differences between male and female phalluses are observed. In males, mesenchyme begins to invade the ventral-proximal GT, thereby partially closing the proximal urethral meatus and separating the definitive PHUR from the surface ectoderm in a proximal-distal wave that continues until postnatal stages (Seifert et al., 2008). This event is thought to occur by fusion of the mesenchymal urethral folds, although invasion by mesenchyme from the perineum has also been proposed (Baskin et al., 2001; Yamada et al., 2003; Seifert et al., 2008). In addition, beginning at E15.5, the distance between the urethral meatus and anus (anogenital distance) is longer in males than in females (Figs 2,3).

Sexual dimorphism becomes more apparent at E16.5 with differentiation of the penis and scrotum in males, as highlighted using *ShhGFP**Cre*;*Rosa26RlacZ* reporter mice (Fig. 3). In males, concurrent with internalisation of the urethra by fusion of the urethral folds, the mesenchyme of the preputial swellings (termed ‘prepuce’ from E16 onwards) fuses at the ventral midline, also in a proximal-distal wave. As the prepuce continues to expand, it envelops the glans (Fig. 3G–L). Mesenchyme fusion at the ventral midline of the GT and remodelling of the urethra result in an indentation on the external surface, called the preputial seam (Fig. 3M–O; Baskin et al., 2001; Yamada et al., 2003; Seifert et al., 2008).

The proximal urethral meatus is nearly closed in males by E16.5, whereas it remains open at the GT/clitoris base in females (Fig. 3; Baskin et al., 2004; Seifert et al., 2008; Wang et al., 2011; Guo et al., 2014). At E17, the GT has differentiated sufficiently to be recognised as the penis/clitoris, and the PHUR becomes the penile urethra in males. Mesenchymal growth also results in a bend in the male urethra at the glans-body junction, which is prominent from E17 and results in

the glans penis being positioned at a right angle bend to the body of the penis (Fig. 3; Cunha and Baskin, 2004; Rodriguez et al., 2011). By contrast, the female urethra is more linear and positioned ventral to the clitoris (Fig. 3A–T).

In females, the UPE can still be seen at E17.5, whereas, in males, it is no longer present and the definitive urethral meatus has formed (Fig. 3Q–V). Although the urethra has opened in the distal glans of the male at this stage (Fig. 3U), urethral maturation and internalisation by invading mesenchyme is not complete until postnatal stages (Baskin et al., 2001; Rodriguez et al., 2012). In female mice, the UPE also continues to canalise; however, because the mesenchyme does not internalise the female urethra, it remains ventral to the clitoris. The proximal urethral meatus remains open at the base of the clitoris. By P8, this opening in the proximal urethral meatus has closed (Kurita, 2010), and its prior location will become the site of the vaginal opening.

In recent years, several publications have provided new insights into the postnatal anatomy of murine external genitalia (Rodriguez et al., 2012, 2011; Schlomer et al., 2013; Weiss et al., 2012; Yang et al., 2010). We have modified the ontology to incorporate these findings (supplementary material). In both sexes, mesenchymal condensations develop into bone (os penis/clitoridis). Males develop cartilage and bands of erectile tissue, called corpora cavernosum. The adult male urethra is subdivided into penile, pelvic and prostatic urethra. The structure of the adult penis is illustrated in Fig. 3W–Y. At the distal tip of the adult glans penis is a tapered extension of the os penis called the male urogenital mating protuberance (MUMP; Rodriguez et al., 2011; Weiss et al., 2012). The glans penis is covered with keratinised epidermal spines. It is positioned internally, within the preputial space, and is completely surrounded by the prepuce externally. The prepuce contains the preputial glands, the ducts of which drain into the preputial space. The glans can be exposed when the prepuce is retracted.

The morphology of the adult mouse clitoris has only recently been described in detail (Yang et al., 2010). Like the penis, the clitoris is surrounded by a prepuce containing preputial glands; however, the clitoris is much smaller and is ventrally tethered to the prepuce, as the clitoral epithelial lamina does not completely enclose the clitoris. Because of this anatomy, the urethra resides partially within the preputial mesenchyme and partially within the clitoris. This is in contrast to humans, in which the urethra is not housed within the clitoris but opens proximal and ventral to the clitoris and is circumscribed by the labia minora.

The PLUR becomes sex specific in the ontology from E15 (Fig. 2E and Fig. 4; supplementary material). Circulating androgens in the male initiate seminal vesicle bud formation from the NDs and, from E16, the ducts become the ductus deferens (Fig. 4A–C). Both seminal vesicles and ductus deferens are connected to the UGS ridge via the ND-derived ejaculatory ducts, and disrupting ND development in males results in loss of these structures (Fig. 4C,D; Guo et al., 2011). The male UGS ridge becomes the verumontanum (Fig. 4C,D; Levin et al., 2007; Yucel and Baskin, 2004).

In females, the UGS ridge blocks the patent opening of the NDs to the PLUR, and from E16 on becomes the sinovaginal bulb (SVB, Fig. 4E,F). By E16.5, the caudal paramesonephric ducts have fused and enlarged to become the upper vagina (Fig. 4F–H). By E18, the upper vagina has fused to the SVB and the vagina comprises both the upper vagina and lower vagina or SVB. These are unique structures with different origins and gene expression profiles (Fig. 4H; Drews et al., 2002; Kurita, 2010). The SVB, a solid epithelial cord, is a transient structure only seen during development



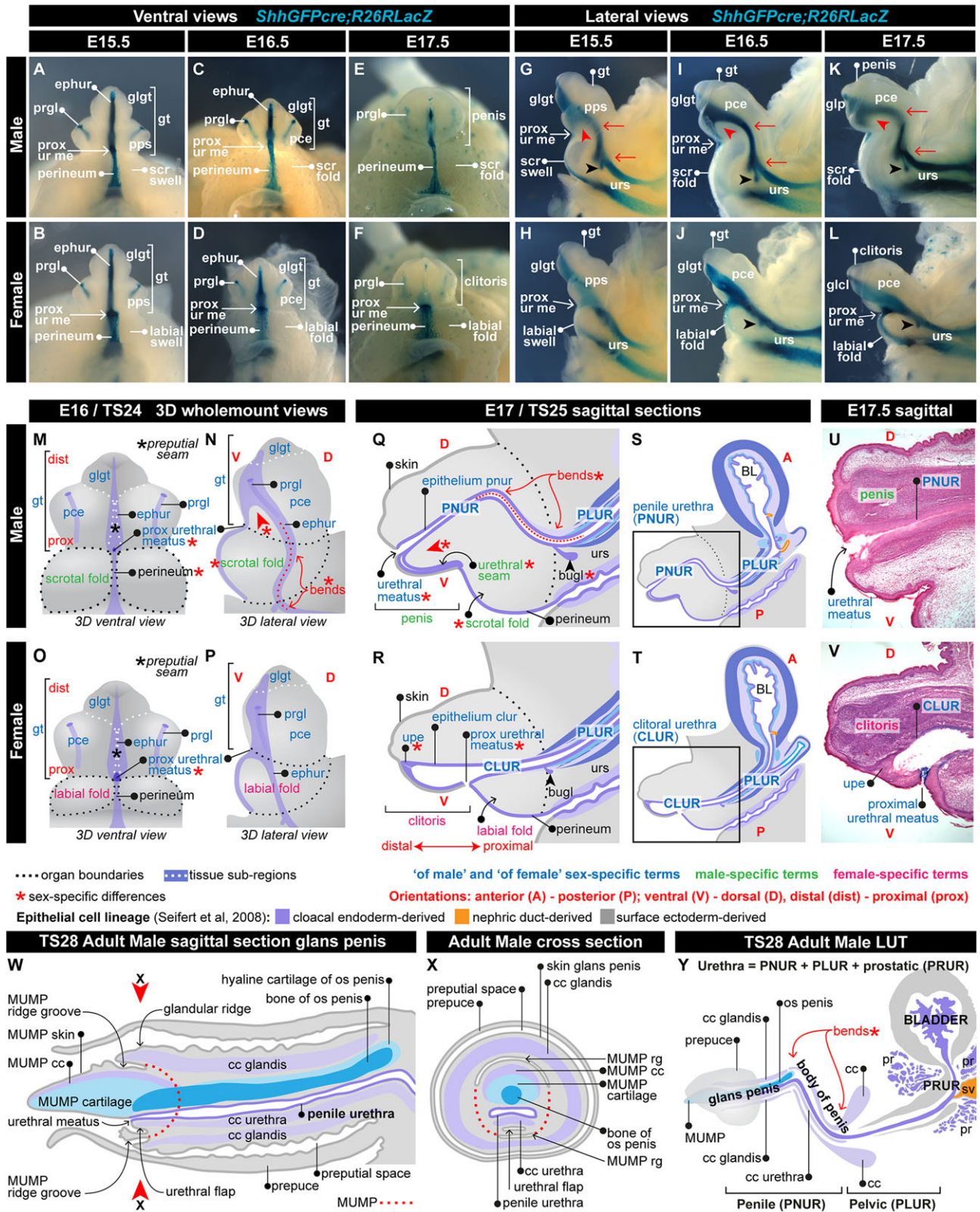


Fig. 3. See next page for legend.

(Kurita, 2010). The upper vagina becomes the adult vagina and the SVB contributes to the vulval epithelium (Kurita, 2010).

Morphological sex differences in the PLUR itself are first seen around E16.5 (Fig. 5; supplementary material). The urethral

epithelium gives rise to accessory glands, including the prostate, bulbourethral glands and numerous urethral glands. Only the prostate glands are male specific. Female bulbourethral glands (new to the ontology), although smaller than the male, are also known as

**Fig. 3. Sexual differentiation of the external genitalia.** (A-L) Whole-mount  $\beta$ -galactosidase staining of *ShhGFP**Cre*;*Rosa26**lacZ* embryos. Descendants of the *Shh*-expressing lineage (blue) contribute to preputial glands, epithelium of PHUR, perineum, rectum/intestine and hair follicles. (M-T) Schematics illustrate external genitalia. From E15.5-17.5 in males, mesenchyme grows distally, the urethra septates (red arrowheads), the proximal urethral meatus closes, the urethral seam forms and two right-angle bends develop in the urethra (red arrows). Male bulbourethral glands (black arrowheads), scrotal swelling/fold and perineum are larger. In both sexes, the preputial seam is seen as an indentation along the prepuce ventral midline (black asterisks in M,O). (U,V) H&E-stained external genitalia sections. (Q-V) At E17.5, the male urethra is patent along its length and open at the urethral meatus; in females, the urethral plate (upe) is present and the urethra opens at the proximal urethra meatus. (W-Y) Schematics illustrating adult male anatomy, showing the male urogenital mating protuberance (MUMP), corpora cavernosa (light purple), cartilage/bone (blue). Red arrowheads (in W) indicate position of cross-section (X). (Y) Two right-angle bends are present in the adult male urethra. The prostatic urethra (PRUR) is surrounded by prostate glands. Paired corpus cavernosum extend anteriorly to join the pubic bone (cc in Y).

Bartholin's glands (Bloomfield, 1927). Like their male counterparts, they are derived from cloacal endoderm and marked by *Shh* (Fig. 2F and Fig. 3G-L).

Prostate gland anatomy is extremely complex (Fig. 5; supplementary material). Several studies describing early murine prostate development (Allgeier et al., 2010, 2009; Cook et al., 2007) have instructed modifications to the ontology. Numerous prostate buds develop from the PLUR epithelium in distinct locations (Fig. 5A-D). Number, size, morphology, location and patterning of the different prostate regions have been described (Allgeier et al., 2010, 2009; Lin et al., 2003; Timms et al., 1994). Bud formation is complete by E18.5 (Lin et al., 2003); however, extensive branching morphogenesis does

not begin until after birth. The glands later develop a patent lumen and the adult prostate secretes a variety of products dependent on region. In adult males, the urethra region surrounded by prostate glands is called the prostatic urethra (Fig. 5I,J).

Urethral glands also form as buds that develop from the PLUR epithelium in both sexes (Fig. 5; supplementary material). Ventral urethral gland buds develop at the male bladder-urethra junction in the same location as ventral prostate buds, but at early stages these are indistinguishable, as both express the early prostatic marker *Nkx3-1* (Allgeier et al., 2010). Consequently, it is difficult to definitively identify any ventral budding structure in the developing male, although there is evidence that *Edar* and *Wnt10b* mRNA staining intensity can separate prostatic gland buds (high expression) from urethral gland buds (low to non-detectable expression; Keil et al., 2012). However, the ontology now includes the indefinite term, ventral epithelial bud, first introduced by Allgeier et al. (2010) (Fig. 5A-H). Female mice can develop functional prostate glands from ventral epithelial buds if exposed to exogenous androgens (Price and Williams-Ashman, 1961; Raynaud, 1938, 1942). In the past, these have been referred to as female prostate buds. The ontology uses ventral epithelial bud in favour of prostate bud for the female mouse. Whereas these buds might go on to form Skene's glands in females, no lineage tracing is available to confirm this and, even in males, not all ventral buds go on to form prostate glands (Allgeier et al., 2010).

#### Regional and cellular updates to the bladder and urethra ontology

In the literature, the bladder has been divided into three different regions: fundus, neck and trigone (supplementary material). We

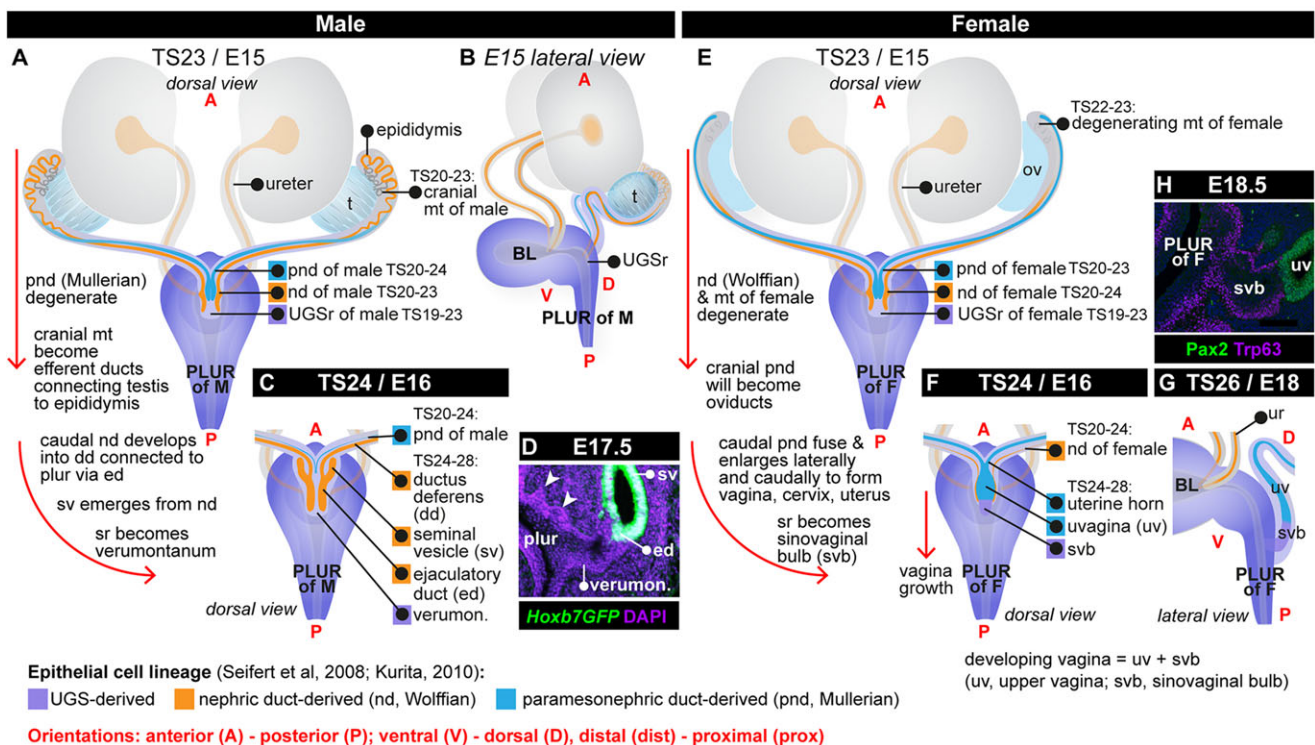


**Fig. 4. Sexual differentiation of the reproductive ducts.** Schematics illustrate 3D anatomy of reproductive ducts and their connection to the PLUR. At E15, the sexes are identical. Red arrows and associated text indicate sex-specific changes. Nephric and paramesonephric duct degeneration is complete by E17.5. (D) Section immunofluorescence of *Hoxb7GFP* embryo shows *Hoxb7GFP*<sup>+</sup> ejaculatory ducts and seminal vesicles. Anterior prostate buds are seen (arrowheads). (F,G) The vagina grows in a posterior direction along the PLUR (red arrow), eventually separating from the PLUR and opening at the base of the clitoris (postnatally). (H) Section immunofluorescence shows differential expression in upper vagina (*Pax2*<sup>+</sup>) and SVB (*Trp63*<sup>+</sup>).



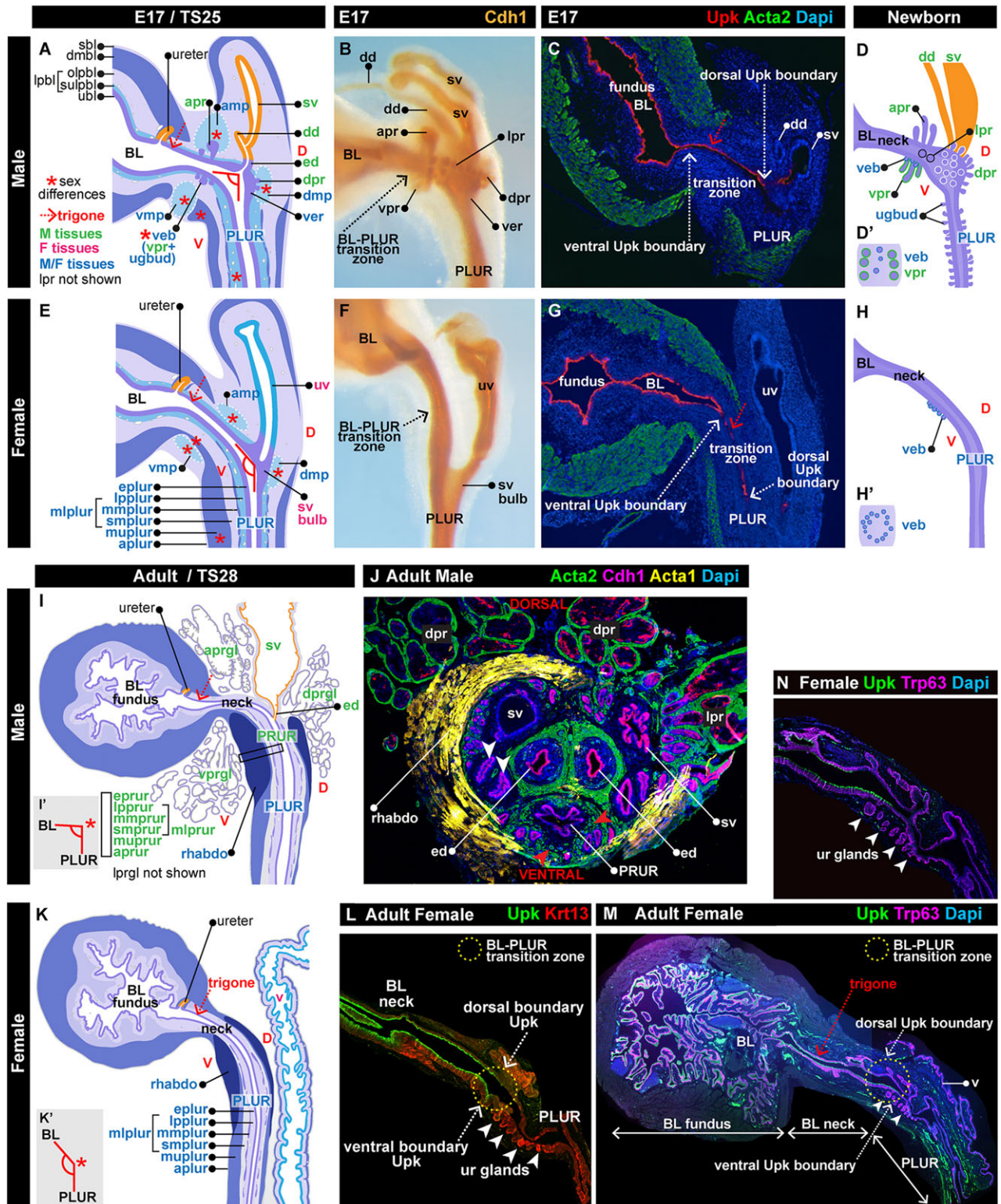


**Fig. 5. Sexual differentiation of the pelvic urethra.** Schematics illustrate sagittal sections of bladder-PLUR junction at E17 (A,E) and adult (I,K). Sex differences (red asterisks) include: mesenchymal pad size/shape; thicker male lamina propria (lpplur) and thicker female muscle (muplur); muscle layer (muplur) continuous with detrusor in females (gap in males); and the bladder-PLUR (BL-PLUR) connection angle, close to 90° in males (I'), more linear in females (K'). (B,F) Whole-mount immunolabelling shows epithelial structures (Cdh1<sup>+</sup>). (C,G) Immunofluorescence of sagittal sections shows smooth muscle (green) and Upk (red) expression. Upk marks the bladder urothelium boundary (dotted arrows). (D,H) 3D illustrations of PLUR epithelium at birth (purple) shows prostate, ventral epithelial and urethral gland bud location; lateral (black), dorsal (white) and ventral (green) prostate glands and ventral epithelial buds (veb, blue) are outlined. (D',H') Underside views of ventral PLUR. (J) Cross-section through adult male PRUR shows labelling of epithelia (red), smooth muscle (green) and striated muscle (yellow), which marks the rhabdosphincter. Blood vessels (Acta2<sup>+</sup>, red arrowheads) and prostate glands (Cdh1<sup>+</sup>, white arrowheads) are seen. (K-N) In female adults, the vagina has elongated and a rhabdosphincter develops. (L-N) Sagittal BL-PLUR sections labelled with Upk (bladder urothelium) shows the adult BL-PLUR transition zone (dotted arrows). Urethral glands (arrowheads, L-N) are located close to the BL-PLUR boundary.



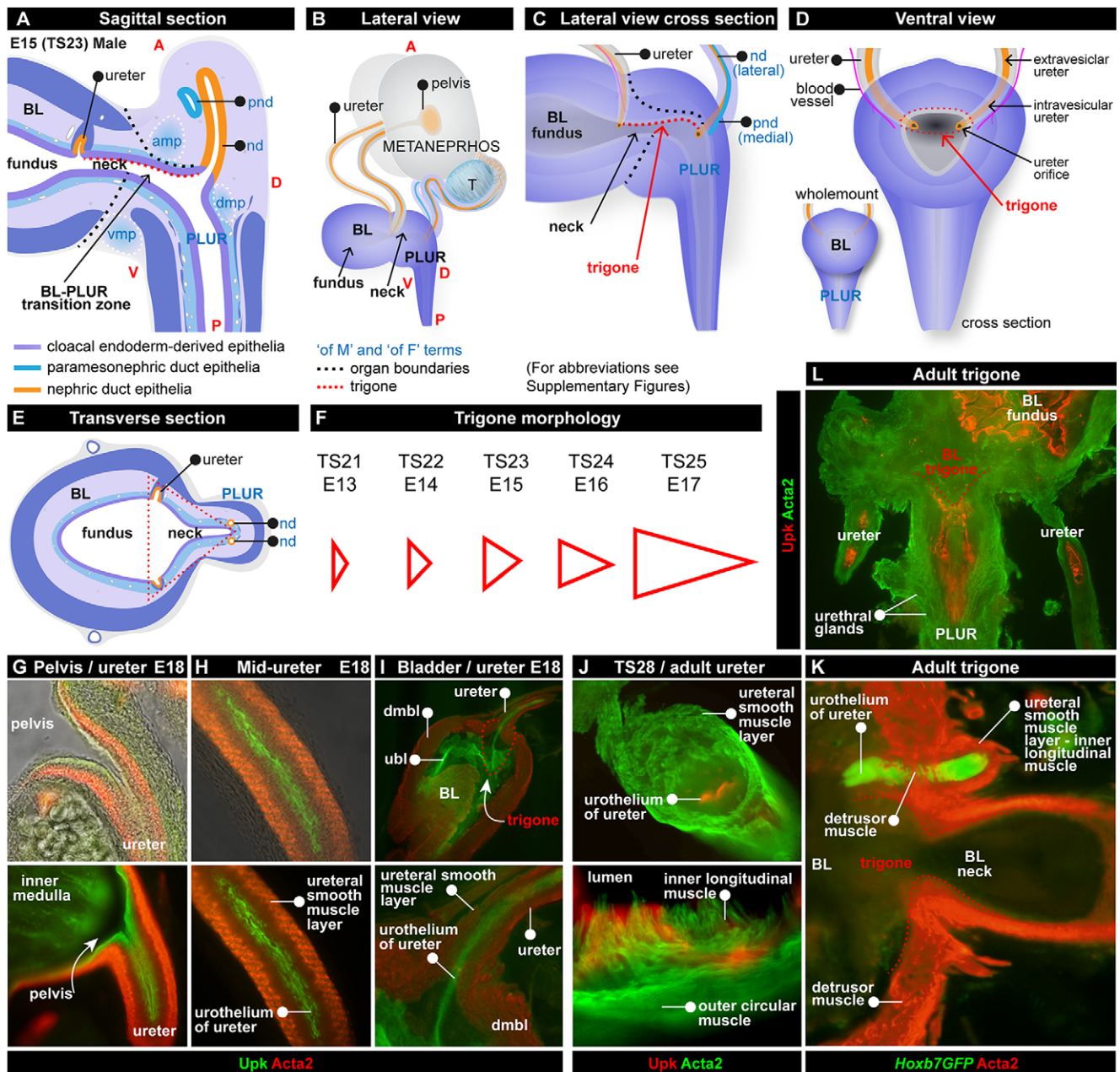


**Fig. 6. Morphology of the bladder fundus, neck, trigone and ureters.** (A-E) Schematics illustrating location and morphology of the bladder regions, ureter and urethra connections at E15. Trigone and BL-PLUR boundaries are shown (red/black dotted lines). The bladder neck is more elongated in the adult (see Fig. 5M). (F) As the bladder grows, trigone morphology changes from an equilateral to an isosceles triangle. (G-L) Immunofluorescence of vibratome sections and whole-mounts of E18 ureter (G-I), adult ureter (J) and trigone (K,L), with labelling of urothelium (Upk), ureter muscle layer and detrusor muscle (Acta2) and *Hoxb7-GFP* in ureter urothelium (K). Approximate trigone boundary is shown (red dotted lines in I,K,L).

have reviewed the definition of these regions and modified the ontology as a result. Anatomically, the bladder is divided into the fundus (or dome), the rounded blind-end of the bladder and the neck, which is the narrow open end of the bladder located between the ureter orifices and the PLUR opening (Figs 5 and 6). The dorsal bladder neck forms a triangular-shaped region called the trigone. The ureter orifices form the trigone base and the urethra opening forms the apex (Fig. 6E). Trigone morphology changes as the bladder and urethra expand, increasing the distance between the ureters and urethral opening (Fig. 6F) (Carpenter et al., 2012). The ureters are muscular tubes that transport urine from the renal pelvis to the bladder (Fig. 6G-J;

supplementary material). The ureters are inserted in a stereotypical position in the trigone, where ureteral muscle and bladder muscle intersect to form the anti-reflux valve (Carpenter et al., 2012; Viana et al., 2007) (Fig. 6K,L).

The bladder urothelium is lined by an apical barrier of urothelial plaque, composed of uroplakin family proteins (Upk1a, Upk1b, Upk2, Upk3a and Upk3b). Expression of multiple Upk proteins is required to create the plaque. The urethra epithelium does not produce uroplakin plaque and therefore has not been described as an urothelium. However, both epithelia are derived from cloacal endoderm, and the exact location of the bladder-urethra boundary is not precise. In the adult, the distribution of urothelial plaque and



Upk protein expression may be used to determine the boundary (Fig. 5L,M). However, during development, Upk expression not only differs between stages, but also differs between dorso-ventral surfaces (Fig. 5C,G). During early development (E11.5-13.5), we have defined the bladder-urethra boundary as the site where the reproductive ducts insert into the urethra (Fig. 1). Later in development, as the ducts differentiate, this boundary becomes difficult to define, especially in the female, when the SVB and vagina move caudally. In order to facilitate the annotation of gene expression within this region at later stages, and at early stages when the reproductive ducts are not visible, we have introduced the term bladder-urethra transition zone, from E11.5 to adult. This zone (Figs 5 and 6) marks the region where these two different epithelia meet and is similar to transitional zones in other organs, such as the female cervix and the oesophagus Z-line.

The bladder is able to stretch to store urine and to contract under autonomic control to expel urine via the urethra. These dynamic movements are facilitated by the detrusor muscle, which is composed of irregularly oriented smooth-muscle fibre bundles that, together with the urothelium, expand and contract in response to stretching. Correct patterning and differentiation of bladder smooth muscle is therefore crucial for bladder function. The muscle forms via interactions between the urothelium and surrounding mesenchyme (Cunha, 1999). Recent studies of environmental factors, epithelial-to-mesenchymal interactions and signalling pathways required for bladder smooth muscle formation have advanced our understanding of this developmental process (Cao et al., 2008, 2010; Cheng et al., 2008; DeSouza et al., 2013; Haraguchi et al., 2007; Liu et al., 2010; Shiroyanagi et al., 2007; Tasian et al., 2010). We have updated the bladder ontology to incorporate these findings (Fig. 7).

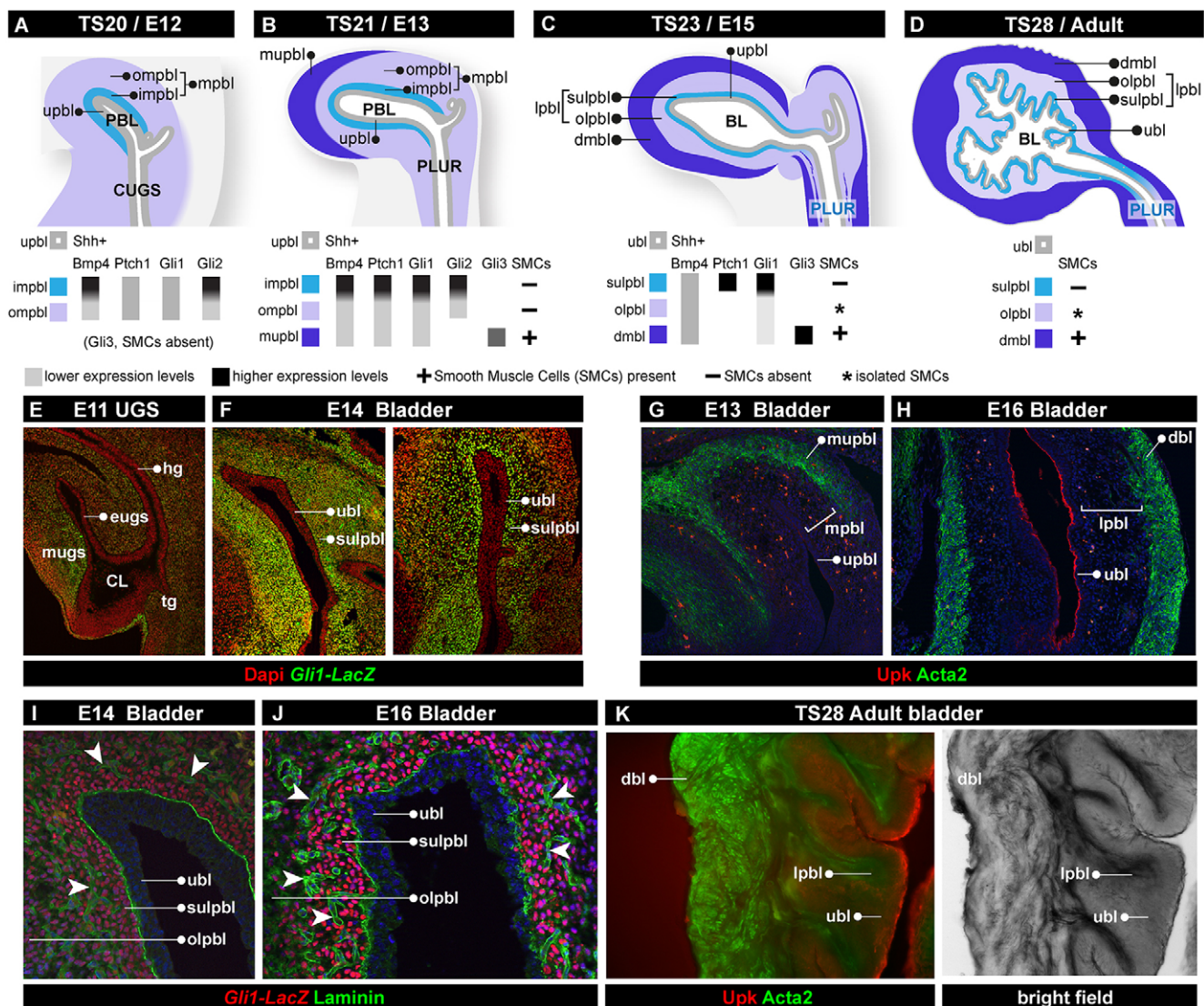


**Fig. 7. Radial patterning of the bladder mesenchyme activates and maintains smooth muscle differentiation.** (A-D) Schematics illustrate mesenchymal and smooth muscle layers. The urothelium expresses *Shh*, signalling the mesenchyme to express *Bmp4*, *Ptch1* and *Gli1-3*. Relative gene expression (lower-higher) and presence/absence of smooth muscle cells are shown. Muscle differentiation begins at the fundus and progresses towards the PLUR (B,C). (E,F)  $\beta$ -galactosidase-labelled *Gli1-lacZ* tissue sections show differential *Gli1* expression in the UGS and bladder mesenchyme. (G,H) Immunolabelled bladder sections show urothelium (Upk) and smooth muscle (Acta2). (I,J)  $\beta$ -galactosidase-labelled *Gli1-lacZ* tissue sections show location of *Gli1* and Laminin. Expression of *Gli1* is strongest in the suburothelial lamina propria (sulpbl) at E14 (I) and E16 (J) and weak or absent in the outer lamina propria (olpbl). The sulpbl also contains numerous blood vessels (Laminin<sup>+</sup>, white arrowheads, I,J). (K) Immunolabelled vibratome sections show urothelium (Upk) and detrusor muscle (Acta2). Bright field (on the right) shows the convoluted adult bladder urothelium.



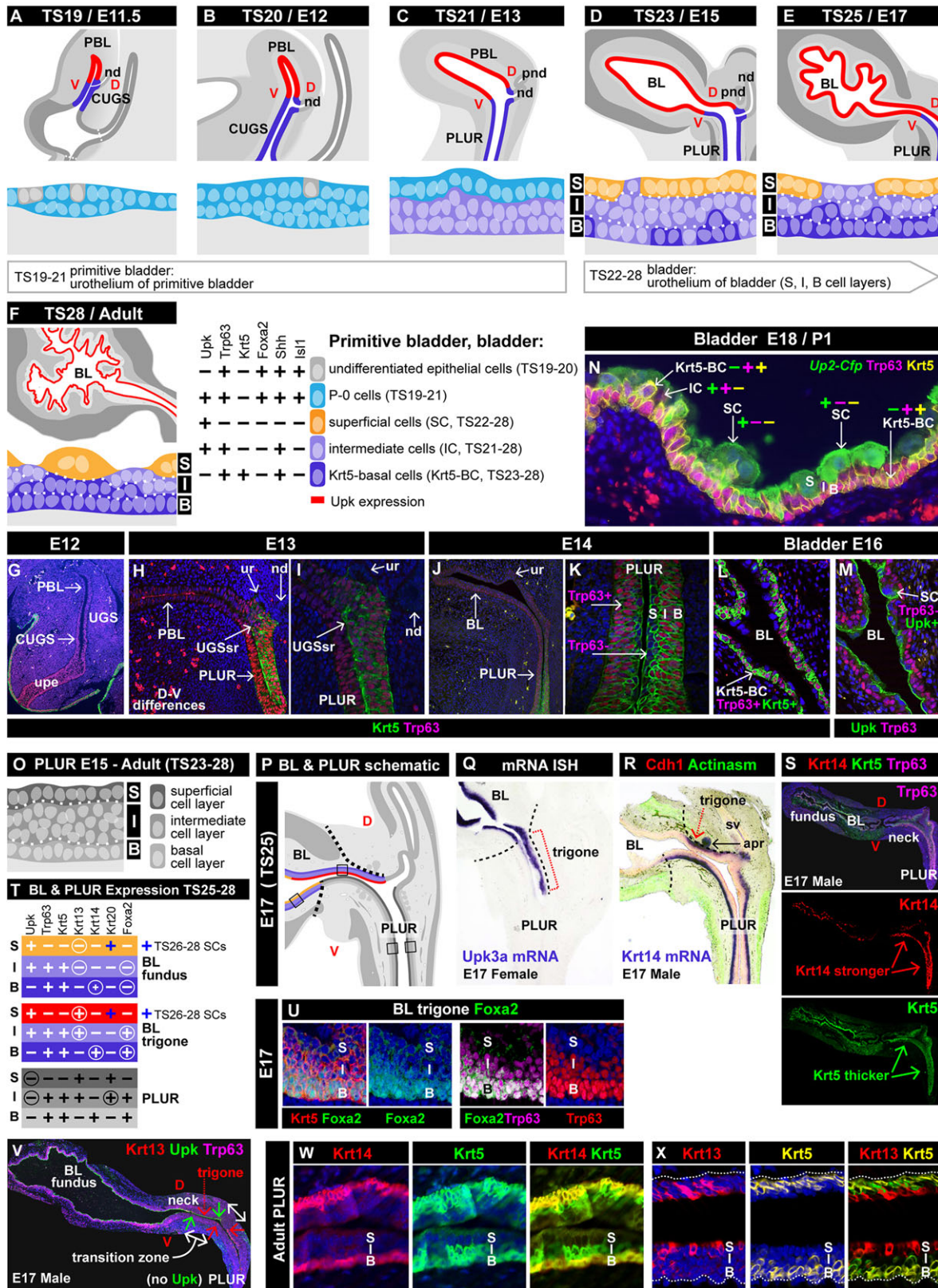


Fig. 8. See next page for legend.

Differentiation of smooth muscle cells from the bladder mesenchyme begins at E13.5 in the outer peripheral zone of the primitive bladder and progresses inwards towards the urothelium. Differentiation is dependent on *Shh* signalling from the cloacal

endoderm-derived epithelium to the surrounding mesenchyme, which upregulates target genes, including *Bmp4*, *Ptch1* and *Gli1*, although their expression is seen much earlier, in the peri-cloacal mesenchyme at E10.5 (Cao et al., 2010; Cheng et al., 2008;



**Fig. 8. Protein expression defines the bladder urothelium and PLUR epithelium cell types.** (A-F) Schematics illustrate epithelial layers; urothelium (red) and caudal UGS (CUGS)/PLUR epithelium (blue). Cross-sections below each panel illustrate location and gene expression of urothelial cell types. (D-F) From E14, bladder urothelium is divided into superficial (S), intermediate (I) and basal (B) cell layers. (G-N) Immunolabelling of LUT tissues. Expression of Trp63 is stronger in CUGS at E12 (G). Krt5 is not expressed in the bladder until after E14; however, expression is seen in the dorsal PLUR epithelium at E13 (H,I), which also shows stronger Trp63 expression. The PLUR superficial cell layer does not express Trp63 at E14 (J,K). (L-N) In the E16 (L,M) and E18 (N) urothelium, Upk is expressed by superficial (SC) and intermediate (IC) cells. Trp63 by ICs and Krt5-basal cells (BCs), and Krt5 exclusively by Krt5-BCs; however, these cells are found in both the basal and intermediate layers. By birth, SCs (or umbrella cells) are large and multi-nucleated (N). *Up2-Cfp* reporter mice show *Upk*-expressing cells (green, N). (O-X) Expression patterns in PLUR versus bladder regions (trigone, red dotted lines/arrows). (O) From E15, the PLUR epithelium is subdivided into superficial (S), intermediate (I) and basal (B) cell layers (S), which are thicker than the bladder urothelium. (P) Schematic shows bladder fundus/ventral neck (yellow), bladder dorsal neck/trigone (red) and PLUR epithelium (grey). (Q) All bladder regions express *Upk*. (R) *Krt14* expressed in bladder neck/trigone and PLUR at E17. (S,U-X) Immunolabelling in the BL-PLUR. (S) Krt14, Krt5 and Trp63 expression. (T) Summary of BL-PLUR expression profiles in the cell layers from E17 to adult (TS25-28). White circles indicate differences between bladder regions; black circles indicate differences between PLUR and bladder. Krt20 is expressed by mature SCs of the bladder from E18 to adult (blue '+' in T). (U) *Foxa2* is expressed in bladder neck/trigone (U) and PLUR, but absent in the bladder fundus (data not shown). (V) E17 BL-PLUR showing tissue regions. Upk (green arrows) and Krt13 (red arrows) expression borders, with BL-PLUR transition zone in between (white arrows). (W,X) Adult PLUR showing Krt14, Krt5 and Krt13 expression in the epithelial layers.

DeSouza et al., 2013; Haraguchi et al., 2007; Liu et al., 2010; Shiroyanagi et al., 2007; Tasian et al., 2010; Suzuki et al., 2012). Fig. 7A-D summarises the relative expression levels of genes in the mesenchyme from E12-15. In the primitive bladder, the strongest expression is seen in a thin layer of the mesenchyme immediately underneath the urothelium, resulting in radial patterning of the mesenchyme. This sub-urothelial layer remains devoid of smooth muscle cells throughout development (Cao et al., 2008, 2010; Shiroyanagi et al., 2007; Fig. 7). We have used *Gli1-lacZ* reporter mice to illustrate this radial patterning (Fig. 7E,F,I,J). The mesenchyme also shows differential cell proliferation between inner and outer layers, also regulated by *Shh* (Tasian et al., 2010), and the inner layer contains numerous blood vessels (Fig. 7I,J). As a result of these findings, the primitive bladder mesenchyme (E12-13) has been subdivided into inner and outer layers (Fig. 7A,B). As smooth muscle cells are detectable at E13.5, before a distinct detrusor muscle is recognised, we have added muscle layer of primitive bladder (Fig. 7B,G). Smooth muscle cells express *Tgfb1* and *Myocd*, together with smooth muscle actins and myosins. Actin alpha-smooth muscle (*Acta2*) is utilised as a marker of early differentiation (Fig. 7G,H,K) and smooth muscle heavy chain myosin (*Myh11*) marks more advanced differentiation (Cheng et al., 2008; DeSouza et al., 2013; Liu et al., 2010; Shiroyanagi et al., 2007).

From E14 to adult, the bladder is composed of urothelium, lamina propria and detrusor muscle, surrounded by either serosa or adventitia, depending on location (Fig. 7 and Fig. 9B). The lamina propria is also subdivided into suburothelial and outer lamina propria layers (Fig. 7C,D,H-K). *Shh* signalling from the urothelium continues throughout development, and genetic markers of the primitive bladder inner mesenchyme maintain their expression in the suburothelial lamina propria of the bladder (Fig. 7A-D). An absence of smooth muscle cells continues to be characteristic of the suburothelial layer through to adult.

The 3D pattern of detrusor muscle differentiation in the mouse bladder has also recently been analysed (Carpenter et al., 2012). Differentiation begins in the distal fundus and advances towards the bladder neck (Fig. 7B). As development progresses and the bladder grows in size, the percentage of urothelium remains constant, whereas the percentage of lamina propria decreases as the outer mesenchyme differentiates into smooth muscle cells of the detrusor.

A smooth muscle layer also differentiates from the PLUR mesenchyme. Unlike the bladder, PLUR mesenchyme does not form a thick muscular layer and was therefore not subdivided into inner and outer layers. There is some evidence that testosterone and oestradiol control smooth muscle differentiation in PLUR of rats and mice (Chrisman and Thomson, 2006; Thomson et al., 2002), and *TGF $\beta$*  signalling might also play a role (Tomlinson et al., 2004). At E13.5, the PLUR is composed of an epithelium, mesenchyme and outer adventitia and, at E14.5, develops a muscle layer. From E15.5 to adult, the mesenchymal layer further differentiates into a thin lamina propria, discontinuous muscularis mucosa (containing smooth muscle cells) and underlying submucosa (Fig. 5 and Fig. 9C). Recent gene expression analysis in the E17 PLUR has provided many markers to distinguish these tissue layers (Abler et al., 2011a). Originally, the terms 'muscularis mucosa' and 'muscularis submucosa' were present in bladder ontology. However, unlike the PLUR, the mouse bladder does not contain a distinct muscularis layer and therefore these layers have been removed.

Late during development, the rhabdosphincter, another muscular structure, which is new to the ontology, develops in the PLUR of both sexes (Fig. 5I-K). The development of this structure is important for normal function of the urinary tract in mice and humans, because decreased sphincter tone and/or thickness, especially in aging multiparous women, has been associated with stress urinary incontinence (Athanasίου et al., 1999; Rortveit et al., 2003). Urethral sling and pelvic mesh surgeries to repair stress urinary incontinence are often ineffective and can lead to complications. Regenerative therapies involving stem cells are a hot research topic as an alternative to these therapies, and understanding sphincter muscle lineage is therefore central to these studies. This suggests a need for lineage studies to define the rhabdosphincter origin. Striated muscle cells develop in the anterior PLUR forming the rhabdosphincter (Borirakchanyavat et al., 1997), which is marked by actin  $\alpha$ -skeletal muscle expression (*Acta1*, Fig. 5J). Although seen in the mouse at E17 (E.M.S.-S., unpublished data) and in rats at birth (Borirakchanyavat et al., 1997), the stage at which the rhabdosphincter forms in the mouse is not known.

#### Marker expression and lineage analyses define cell types in the bladder urothelium and urethra epithelium

The adult bladder urothelium is stratified, containing a basal layer of Krt5-expressing basal cells (Krt5-BCs), one or more layers of intermediate cells (ICs), and a superficial (or luminal) layer of superficial cells (SCs) (Gandhi et al., 2013). Lineage analysis in mouse suggests that ICs are progenitors that self-renew and generate SCs in the adult, whereas, during development, P-0 cells, a newly identified population undetectable in the adult, serve as transient progenitors that generate ICs and SCs in the embryo (Gandhi et al., 2013). The bladder urothelial ontology has been revised to include cell types, while retaining urothelial layers. This enables the annotation of data without knowing the cell type, and allows for the incorporation of data from previous publications referring to layer.

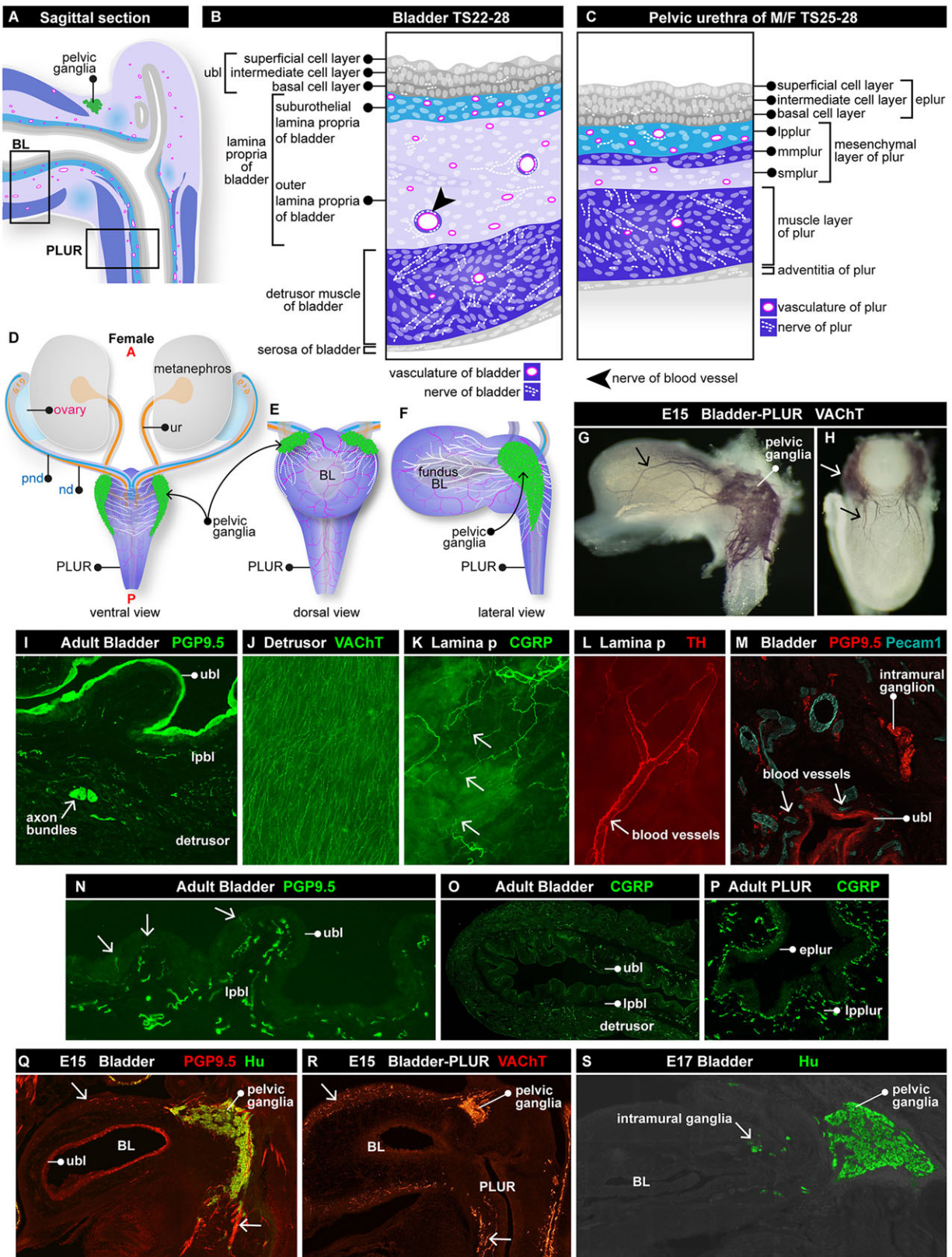


Fig. 9. See next page for legend.

Urothelial cell types have been defined by marker expression and relative position (Gandhi et al., 2013). During development, the cellular composition of the urothelial layers changes considerably (Fig. 8A-M; supplementary material). The urothelium expresses a

series of endodermal markers (Shh, Trp63, Isl1, Foxa2). From E11-12, a small number of endodermal epithelial cells ( $Upk^{-}$ ) are seen; however, most of the primitive bladder is lined by P-0 cells, transient progenitors expressing  $Upk$  and endodermal markers but



**Fig. 9. Nerves, pelvic ganglia and vasculature of the LUT.** (A–F) E15 schematics illustrate nerves, pelvic ganglia (green) and vasculature. Pelvic ganglia extend their processes towards the PLUR midline (D) and bladder fundus (E,F). Only small areas of pelvic ganglia are visible in midline sagittal sections (A). (B,C) Bladder (E14 to adult) and PLUR (E17 to adult) ontology terms. Nerves are present in each tissue layer, in addition to nerves of blood vessels (arrowhead, B). (G,H) Whole-mount bladder-PLUR immunolabelled for VACHT show pelvic ganglion (white arrow), with axonal processes extending towards the bladder fundus (black arrows). (I) The pan-neuronal marker PGP9.5 labels axons, axon bundles (white arrow) and urothelial superficial cells in transverse section. (J) VACHT, marking cholinergic autonomic axons, labels varicose axons in whole-thickness adult detrusor. (K) CGRP marks a major population of sensory axons in whole-thickness lamina propria of adult bladder (focusing on suburothelial lamina propria). Arrows indicate terminating axons. (L) Tyrosine hydroxylase marking noradrenergic autonomic axons in whole-thickness lamina propria of adult bladder showing blood vessel innervation. (M) Pecam1-labelled vasculature (vascular endothelial cells) beneath the adult urothelium (PGP9.5<sup>+</sup>). Clustered PGP9.5<sup>+</sup> neuronal cell bodies form an intramural ganglion. (N,O) CGRP-labelled sensory axons form a network in the lamina propria, especially the suburothelial region (transverse section). Usually terminating in basal and intermediate urothelial layers, some axons penetrate the superficial cell layer (arrows, N). CGRP<sup>+</sup> axons show even density in the bladder fundus, but there is an increase in suburothelial axons closer to the bladder neck (right hand of image, O). (P) Anterior PLUR transverse section shows the dense plexus of CGRP<sup>+</sup> sensory axons in the lamina propria. (Q–S) BL-PLUR sagittal sections showing pelvic ganglia. At E15, neuronal bodies (Hu<sup>+</sup>) within pelvic ganglia begin segregating into distinct clusters. Axonal processes (PGP9.5<sup>+</sup>) extend towards the bladder fundus and distal urethra (arrows, Q). VACHT immunolabelling highlights nerve fibre density and penetration, showing axons in the distal bladder fundus and PLUR (arrows, R). At E15, nerve fibres have not penetrated the detrusor. By contrast, urethral innervation is denser and close to the epithelium (R). At E17, clusters of Hu<sup>+</sup> neuronal bodies are evident within intramural ganglia of the bladder neck (S).

not Krt5 (C.M., unpublished data). By E13, ICs make up most of the urothelium.

From E14, the ontology subdivides urothelium into superficial, intermediate and basal cell layers (Fig. 8A–M). By E14, the basal layer is lined with ICs and the superficial layer mostly with SCs. The intermediate layer consists solely of ICs until E13. Krt5-BCs, first identified between E14 and E15, are seen in intermediate and basal layers. By E17, they line the entire basal layer, displacing ICs to the intermediate layer. In the adult, Krt5-BCs make up 90% of the urothelium, whereas ICs and SCs each make up 5% (Gandhi et al., 2013). Interestingly, our analysis suggests that a second Krt5-BC population (Krt5<sup>+</sup>, Krt14<sup>+</sup>, Trp63<sup>+</sup>) emerges after E17 (C.M., unpublished data). Krt5-BC populations self-renew (Colopy et al., 2014) and are known to arise from cloacal endoderm; however, whether they have a distinct progenitor in the bladder is unclear.

Early in development, the UPE, primitive bladder and caudal UGS all express Shh, Trp63, Isl1 and Foxa2. Trp63 expression is shown in the bladder-PLUR (Fig. 8G–K). Krt5, a marker of Krt5-BCs in the bladder urothelium, is also expressed by the PLUR (Fig. 8H–K). Although not expressed by the bladder until after E14, it is seen as early as E12 in the caudal UGS (Fig. 8G) and UGS ridge at early stages (Fig. 8H,I).

Like the urothelium, the PLUR epithelium is stratified and, from E15, has been subdivided into superficial, intermediate and basal cell layers (Fig. 8O,P). We have used protein expression analysis to examine the distinct cell types that populate the PLUR epithelium compared with the bladder neck/trigone and fundus (Fig. 8). The PLUR basal cell layer is populated by cells expressing Trp63, Krt5, Krt14 and Foxa2. A second cell type (Trp63<sup>+</sup>, Krt5<sup>+</sup>, Foxa2<sup>+</sup>, Krt14<sup>-</sup>, Krt13<sup>+</sup>) resides in the intermediate layer, and the superficial

layer is populated by a third cell type (Trp63<sup>-</sup>, Krt5<sup>-</sup>, Krt14<sup>-</sup>, Foxa2<sup>-</sup>, Krt13<sup>+</sup>). *Kremen1* expression marks the PLUR intermediate and basal cell layers at E17 (Abler et al., 2011a). As is the case with bladder Krt5-BCs, the lineage of these PLUR cell types is not clear; however, these cells persist into adulthood (Fig. 8W,X).

The epithelium transitions from bladder urothelium to PLUR epithelium. Even late in development, there is a distinct zone where the epithelium transitions (Fig. 8V). Between these regions the epithelial expression profile changes. The bladder-PLUR regions are shown at E17 (Fig. 8P–S,V), although the bladder neck is more elongated in the adult (Fig. 5M). PLUR epithelium is thicker than bladder urothelium (see Krt5, Fig. 8S). E17 bladder shows *Upk3a* mRNA and Upk protein in the intermediate and superficial cell layers of the bladder fundus, neck and trigone, but not in the PLUR (Fig. 8Q,V) (Abler et al., 2011a). The PLUR, bladder neck and trigone basal cell layers all strongly express Krt14 (Fig. 8R–T,W), which is weakly expressed by the bladder fundus (Fig. 8S,T). Foxa2 and Krt13 are exclusively expressed by the PLUR, bladder neck and trigone (Fig. 8V,X,U). Therefore, the combined expression patterns of Foxa2, Krt13, Krt14 and Upks can be used to identify distinct epithelial regions (Fig. 8T).

### Nerves, vasculature and pelvic ganglia

The adult lower urogenital tract receives an extensive supply of nerves and vasculature, forming well before birth (supplementary material). In this update, nerves and vasculature have been added as components of the major organs and tissues. In addition, from E15 to adult (TS23–28), nerves of the bladder and PLUR have been described in much more detail and have been added as components of each tissue layer within these organs (Fig. 9). This updated ontology also defines blood vessels within each of the tissue layers so that nerves supplying those vessels can be annotated. However, prior to E15, the ontology has not been updated to the same level of detail. This will require further refinement once innervation and vascularisation of earlier stages and other LUT tissues have been examined more closely.

Numerous developing neural subpopulations have been identified and show distinct patterns of distribution among LUT tissues (Fig. 9I–P). LUT nerves can be sensory or motor (autonomic). Although each should produce distinctive transmitters or related signalling molecules, they are structurally indistinguishable, and no data currently exists on the spatiotemporal distinction between these populations. For this reason, the different types are not distinguished in the ontology. The pelvic ganglia are paired ganglia that develop in the LUT close to the anterior PLUR (Fig. 9D–H,Q–S). They comprise a mixture of both sympathetic and parasympathetic neurons (Keast, 1995; Wanigasekara et al., 2003). The intermixing of sympathetic and parasympathetic neurons within the one ganglion is unique in the autonomic nervous system. In rodents, pelvic ganglia also show considerable sexual dimorphism (Greenwood et al., 1985) (supplementary material).

### DISCUSSION

Presented here is a definitive spatiotemporal description of the developing lower urinary and reproductive tracts, at the level of organ, tissue and, where possible, component cell type. This information has been incorporated into a text-based anatomical ontology spanning developmental time, space and gender. The improved ontology will provide a common language for those in the field, and enable higher resolution annotations of gene and protein expression in the developing and adult lower urogenital tract of both

wild type and genetically altered mouse models. This will in turn facilitate the identification of markers of novel subcompartments at a finer microanatomical resolution. As such, the revised ontology will provide a basis for understanding congenital lower urogenital tract abnormalities commonly seen, but not well understood, in humans.

## MATERIALS AND METHODS

### Literature review

A comprehensive literature review was performed to improve accuracy of the mouse lower urogenital tract ontology from E10.5 to adult (supplementary material). Ontology changes were made based upon this review and group consensus of the authors.

### Modifications to the GUDMAP ontology

The structure and principles of the GUDMAP ontology have been described (supplementary material; Little et al., 2007). The updated ontology and definitions (including features, synonyms, molecular markers and lineage relationships where established) are available on the GUDMAP website (<http://www.gudmap.org/Resources/Ontology/index.php>). The ontology has been entered into the EMAP mouse embryo ontology (Hayamizu et al., 2013) and published on the Open Biological and Biomedical Ontologies web resource (<http://www.obofoundry.org/>).

### Mouse strains, tissue collection and processing

All procedures involving animals were approved by the relevant animal ethics committees (details in supplementary material, including transgenic staining). Wild-type mice were C57BL/6, C57BL/6J or Swiss Webster. Timed matings were established and foetal tissues collected at stages indicated in the Figures. Adult mice were euthanized by isoflurane overdose or cervical dislocation. Tissues were dissected in phosphate-buffered saline (PBS) and fixed before proceeding to whole-mount methods or sectioning.

### Immunohistochemistry (IHC) and immunofluorescence (IF)

Detailed methods are included as supplementary material. For whole-mount IHC (Fig. 5B,F) (Keil et al., 2012), section IHC (Fig. 8R) (Abler et al., 2011a), E15 whole-mount IHC (Fig. 9G,H) (Wiese et al., 2012) and whole adult bladders (Fig. 9J-L) (Yan and Keast, 2008), tissues were immunostained as described previously.

For IF of tissues from Swiss Webster (Fig. 1D-G, Fig. 2F, Fig. 4H, Fig. 5C,F, J-L, Fig. 6G,H,K, Fig. 7G-J and Fig. 8G-N,S,U-X), *Hoxb7GFP* (Fig. 11-M and Fig. 4D) and *Gli-lacZ* (Fig. 6E,F,I,J) mice, sectioned tissues (paraffin, frozen, vibratome) were pre-treated with 10% HIHS, 0.1% Triton-PBS for 1-2 h (25°C). Antigen retrieval was performed by boiling samples for 30 min. Primary antibodies (in 1% HIHS, 0.1% Triton-PBS) were incubated overnight (4°C). Slides were washed in 0.1% Triton-PBS, incubated with secondary antibodies 1-2 h (25°C), followed by DAPI (5-10 min) and cover-slipped with mounting medium (Dako). Antibodies detecting *Hoxb7-GFP* and *Gli-lacZ* were chicken anti-GFP (AVES, #GFP-1020; 1:300) and goat anti- $\beta$ -galactosidase (Biogenesis, #4600-1409; 1:1000).

For IF of C57BL/6J tissues (Fig. 1H, Fig. 8R and Fig. 5J), 5- $\mu$ m paraffin sections were labelled as described previously (Abler et al., 2011a). In Fig. 5J, two consecutive sections are shown, one stained with anti-Acta1 antibody and DAPI, the other with anti-Cdh1 and anti-Acta2 antibodies. Acta1 staining was pseudo-coloured yellow and the images were merged. For IF (Fig. 9I,N-P,Q-S), cryosections (14-20  $\mu$ m thickness) were processed according to described methods (Yan and Keast, 2008; Wiese et al., 2012).

### Section mRNA *in situ* hybridisation (SISH)

SISH using C57BL/6J E17 tissues (Fig. 8P,R) was conducted as described previously (see supplementary material; Abler et al., 2011a,b). IF (Fig. 8R) was performed post-SISH, using the C57BL/6J protocol described above.

### $\beta$ -galactosidase staining

For  $\beta$ -galactosidase activity detection (Figs 2,3) fixed *ShhGFP*Cre; *Rosa26RlacZ* embryos were washed in *lacZ* buffer (1 M sodium

phosphate pH 7.4, 0.1% sodium deoxycholate, 1 M MgCl<sub>2</sub>, 0.2% NP40). For staining, X-gal (1 mg/ml), K<sub>3</sub>[Fe(CN)<sub>6</sub>] and K<sub>4</sub>[Fe(CN)<sub>6</sub>] (0.05 M) were added to the *lacZ* buffer, and embryos were incubated overnight (25°C). Embryos were washed in PBS and stored in 4% PFA.

### Acknowledgements

The authors would like to thank Michael Wicks (MRC IGMM) for providing assistance with OBO file processing and for implementing the version control system, and Elsbeth Richardson for providing expert cryostat sectioning and immunostaining of nerves in adult mouse bladder. The anti-Hu antibody was a generous gift from Vanda A. Lennon (Department of Laboratory Medicine and Pathology, Mayo Clinic, Rochester, MN, USA). The GUDMAP Database and Website [www.gudmap.org](http://www.gudmap.org) are funded by the National Institutes of Health (NIH).

### Competing interests

The authors declare no competing or financial interests.

### Author contributions

K.M.G., J.A., J.R.K., K.M.M., E.M.S.-S., M.J.C., M.H.L., C.M.V. and C.M. contributed to the conception and design of the manuscript. J.R.K., C.E.L., E.M.S.-S., M.J.C., E.B., H.D., K.S., D.P.B., C.B.W., C.M.V. and C.M. contributed to acquisition of experimental data. K.M.G., J.R.K., C.E.L., K.M.M., E.M.S.-S., M.J.C., E.B., H.D., K.S., D.P.B., C.B.W., C.M.V. and C.M. contributed to analysis and interpretation of data. K.M.G., J.R.K., C.E.L., K.M.M., E.M.S.-S., M.J.C., M.H.L., C.M.V. and C.M. contributed to the preparation and critical revision of the manuscript. K.M.G., J.R.K., C.E.L., E.M.S.-S., C.M.V. and C.M. contributed to figure design. J.A., J.B., J.A.D., S.D.H. and R.A.B. contributed to the implementation of the ontology and associated GUDMAP website data.

### Funding

The research of the authors was supported by the National Institute of Diabetes and Digestive and Kidney Diseases (NIDDK) [grant R01DK085242 to K.M.M.] and National Institutes of Health (NIH) grants [DK070136 to M.H.L.], [DK083425 to C.M.V.], [DK092983 to J.A.D. and R.A.B.], [DK094523 and ES017099 to M.J.C.], [U01 DK094479 to J.R.K.], [R56 DK078158 R01 DK078158 and subcontract on U01 DK070219 to E.M.S.-S.]. M.H.L. is a National Health and Medical Research Council of Australia Senior Principal Research Fellow. Deposited in PMC for release after 12 months.

### Supplementary material

Supplementary material available online at <http://dev.biologists.org/lookup/suppl/doi:10.1242/dev.117903/-/DC1>

### References

- Abler, L. L., Keil, K. P., Mehta, V., Joshi, P. S., Schmitz, C. T. and Vezina, C. M. (2011a). A high-resolution molecular atlas of the fetal mouse lower urogenital tract. *Dev. Dyn.* **240**, 2364-2377.
- Abler, L. L., Mehta, V., Keil, K. P., Joshi, P. S., Flucus, C. L., Hardin, H. A., Schmitz, C. T. and Vezina, C. M. (2011b). A high throughput *in situ* hybridization method to characterize mRNA expression patterns in the fetal mouse lower urogenital tract. *J. Vis. Exp.* **54**, 2912.
- Allgeier, S. H., Vezina, C. M., Lin, T.-M., Moore, R. W., Silverstone, A. E., Mukai, M., Gavalchin, J., Cooke, P. S. and Peterson, R. E. (2009). Estrogen signaling is not required for prostatic bud patterning or for its disruption by 2,3,7,8-tetrachlorodibenzo-p-dioxin. *Toxicol. Appl. Pharmacol.* **239**, 80-86.
- Allgeier, S. H., Lin, T.-M., Moore, R. W., Vezina, C. M., Abler, L. L. and Peterson, R. E. (2010). Androgenic regulation of ventral epithelial bud number and pattern in mouse urogenital sinus. *Dev. Dyn.* **239**, 373-385.
- Athanasios, S., Khullar, V., Boos, K., Salvatore, S. and Cardozo, L. (1999). Imaging the urethral sphincter with three-dimensional ultrasound. *Obstet. Gynecol.* **94**, 295-301.
- Baskin, L. S., Erol, A., Jegatheesan, P., Li, Y., Liu, W. and Cunha, G. R. (2001). Urethral seam formation in hypospadias. *Cell Tissue Res.* **305**, 379-387.
- Baskin, L. S., Liu, W., Bastacky, J. and Yucel, S. (2004). Anatomical studies of the mouse genital tubercle. *Hypospadias Genital Dev.* **545**, 103-121.
- Bloomfield, A. (1927). The development of the lower end of the vagina. *J. Anat.* **62**, 9-32.
- Borirakchanyavat, S., Baskin, L. S., Kogan, B. A. and Cunha, G. R. (1997). Smooth and striated muscle development in the intrinsic urethral sphincter. *J. Urol.* **158**, 1119-1122.
- Cao, M., Liu, B., Cunha, G. and Baskin, L. (2008). Urothelium patterns bladder smooth muscle location. *Pediatr. Res.* **64**, 352-357.
- Cao, M., Tasian, G., Wang, M.-H., Liu, B., Cunha, G. and Baskin, L. (2010). Urothelium-derived Sonic hedgehog promotes mesenchymal proliferation and induces bladder smooth muscle differentiation. *Differentiation* **79**, 244-250.



- Carpenter, A., Paulus, A., Robinson, M., Bates, C. M., Robinson, M. L., Hains, D., Kline, D. and McHugh, K. M. (2012). 3-Dimensional morphometric analysis of murine bladder development and dysmorphogenesis. *Dev. Dyn.* **241**, 522-533.
- Cheng, W., Yeung, C.-K., Ng, Y.-K., Zhang, J.-R., Hui, C.-C. and Kim, P. C. W. (2008). Sonic Hedgehog mediator Gli2 regulates bladder mesenchymal patterning. *J. Urol.* **180**, 1543-1550.
- Ching, S. T., Cunha, G. R., Baskin, L. S., Basson, M. A. and Klein, O. D. (2014). Coordinated activity of Spry1 and Spry2 is required for normal development of the external genitalia. *Dev. Biol.* **386**, 1-11.
- Chrisman, H. and Thomson, A. A. (2006). Regulation of urogenital smooth muscle patterning by testosterone and estrogen during prostatic induction. *Prostate* **66**, 696-707.
- Colopy, S. A., Bjorling, D. E., Mulligan, W. A. and Bushman, W. (2014). A population of progenitor cells in the basal and intermediate layers of the murine bladder urothelium contributes to urothelial development and regeneration. *Dev. Dyn.* **243**, 988-998.
- Cook, C., Vezina, C. M., Allgeier, S. H., Shaw, A., Yu, M., Peterson, R. E. and Bushman, W. (2007). Noggin is required for normal lobe patterning and ductal budding in the mouse prostate. *Dev. Biol.* **312**, 217-230.
- Cunha, G. R. (1975). Hormonal influences on the morphogenesis of the preputial gland of embryonic mice. *Anat. Rec.* **181**, 35-53.
- Cunha, G. R. (1999). Overview of epithelial-mesenchymal interactions in the bladder. *Adv. Exp. Med. Biol.* **462**, 3-5.
- Cunha, G. R. and Baskin, L. (2004). Development of the penile urethra. *Adv. Exp. Med. Biol.* **545**, 87-102.
- DeSouza, K. R., Saha, M., Carpenter, A. R., Scott, M. and McHugh, K. M. (2013). Analysis of the Sonic Hedgehog signaling pathway in normal and abnormal bladder development. *PLoS ONE* **8**, e53675.
- Dreus, U., Sulak, O. and Schenck, P. A. (2002). Androgens and the development of the vagina. *Biol. Reprod.* **67**, 1353-1359.
- Gandhi, D., Molotkov, A., Batourina, E., Schneider, K., Dan, H., Reiley, M., Laufer, E., Metzger, D., Liang, F., Liao, Y. et al. (2013). Retinoid signaling in progenitors controls specification and regeneration of the urothelium. *Dev. Cell* **26**, 469-482.
- Glenister, T. W. (1954). The origin and fate of the urethral plate in man. *J. Anat.* **88**, 413-425.
- Greenwood, D., Coggeshall, R. E. and Hulsebosch, C. E. (1985). Sexual dimorphism in the numbers of neurons in the pelvic ganglia of adult rats. *Brain Res.* **340**, 160-162.
- Guioli, S., Sekido, R. and Lovell-Badge, R. (2007). The origin of the Mullerian duct in chick and mouse. *Dev. Biol.* **302**, 389-398.
- Guo, Q., Tripathi, P., Poyo, E., Wang, Y., Austin, P. F., Bates, C. M. and Chen, F. (2011). Cell death serves as a single etiological cause of a wide spectrum of congenital urinary tract defects. *J. Urol.* **185**, 2320-2328.
- Guo, C., Sun, Y., Guo, C., MacDonald, B. T., Borer, J. G. and Li, X. (2014). Dkk1 in the peri-cloaca mesenchyme regulates formation of anorectal and genitourinary tracts. *Dev. Biol.* **385**, 41-51.
- Haraguchi, R., Motoyama, J., Sasaki, H., Satoh, Y., Miyagawa, S., Nakagata, N., Moon, A. and Yamada, G. (2007). Molecular analysis of coordinated bladder and urogenital organ formation by Hedgehog signaling. *Development* **134**, 525-533.
- Hayamizu, T. F., Wicks, M. N., Davidson, D. R., Burger, A., Ringwald, M. and Baldock, R. A. (2013). EMAP/EMAPA ontology of mouse developmental anatomy: 2013 update. *J. Biomed. Semantics* **4**, 15.
- Keast, J. R. (1995). Visualization and immunohistochemical characterization of sympathetic and parasympathetic neurons in the male rat major pelvic ganglion. *Neuroscience* **66**, 655-662.
- Keil, K. P., Mehta, V., Ablner, L. L., Joshi, P. S., Schmitz, C. T. and Vezina, C. M. (2012). Visualization and quantification of mouse prostate development by in situ hybridization. *Differentiation* **84**, 232-239.
- Kurita, T. (2010). Developmental origin of vaginal epithelium. *Differentiation* **80**, 99-105.
- Levin, T. L., Han, B. and Little, B. P. (2007). Congenital anomalies of the male urethra. *Pediatr. Radiol.* **37**, 851-862; quiz 945.
- Lin, T.-M., Rasmussen, N. T., Moore, R. W., Albrecht, R. M. and Peterson, R. E. (2003). Region-specific inhibition of prostatic epithelial bud formation in the urogenital sinus of C57BL/6 mice exposed in utero to 2,3,7,8-tetrachlorodibenzo-p-dioxin. *Toxicol. Sci.* **76**, 171-181.
- Lin, C., Yin, Y., Veith, G. M., Fisher, A. V., Long, F. and Ma, L. (2009). Temporal and spatial dissection of Shh signaling in genital tubercle development. *Development* **136**, 3959-3967.
- Little, M. H., Brennan, J., Georgas, K., Davies, J. A., Davidson, D. R., Baldock, R. A., Beverdam, A., Bertram, J. F., Capel, B., Chiu, H. S. et al. (2007). A high-resolution anatomical ontology of the developing murine genitourinary tract. *Gene Expr. Patterns* **7**, 680-699.
- Liu, B., Feng, D., Lin, G., Cao, M., Kan, Y. W., Cunha, G. R. and Baskin, L. S. (2010). Signalling molecules involved in mouse bladder smooth muscle cellular differentiation. *Int. J. Dev. Biol.* **54**, 175-180.
- Miyagawa, S., Harada, M., Matsumaru, D., Tanaka, K., Inoue, C., Nakahara, C., Haraguchi, R., Matsushita, S., Suzuki, K., Nakagata, N. et al. (2014). Disruption of the temporally regulated cloaca endodermal  $\beta$ -catenin signaling causes anorectal malformations. *Cell Death Differ.* **21**, 990-997.
- Ng, R. C.-L., Matsumaru, D., Ho, A. S.-H., Garcia-Barceló, M.-M., Yuan, Z.-W., Smith, D., Kodjabachian, L., Tam, P. K.-H., Yamada, G. and Lui, V. C.-H. (2014). Dysregulation of Wnt inhibitory factor 1 (Wif1) expression resulted in aberrant Wnt-beta-catenin signaling and cell death of the cloaca endoderm, and anorectal malformations. *Cell Death Differ.* **21**, 978-989.
- Nievelstein, R. A. J., van der Werff, J. F. A., Verbeek, F. J., Valk, J. and Vermeij-Keers, C. (1998). Normal and abnormal embryonic development of the anorectum in human embryos. *Teratology* **57**, 70-78.
- Orvis, G. D. and Behringer, R. R. (2007). Cellular mechanisms of Müllerian duct formation in the mouse. *Dev. Biol.* **306**, 493-504.
- Perritt, C. L., Powles, N., Chiang, C., Maconochie, M. K. and Cohn, M. J. (2002). Sonic hedgehog signaling from the urethral epithelium controls external genital development. *Dev. Biol.* **247**, 26-46.
- Price, D. and Williams-Ashman, H. (1961). *The Accessory Reproductive Glands of Mammals*. Baltimore: Waverly Press.
- Rasouly, H. M. and Lu, W. (2013). Lower urinary tract development and disease. *Wiley Interdiscip. Rev. Syst. Biol. Med.* **5**, 307-342.
- Raynaud, A. (1938). Intersexualité obtenue expérimentalement chez la souris femelle par action hormonale. [Intersexuality obtained in experiments in the female mouse by hormonal action.]. *Bull. Biol. Fr. Belg.* **72**, 297-354.
- Raynaud, A. (1942). Modification expérimentale de la différenciation sexuelle des embryons de souris par action des hormones androgènes et oestrogènes (première et deuxième parties). [Experimental modification of the sexual differentiation of mouse embryos by action of the hormones androgens and estrogens (first and second parts)]. *Actual Sci. Indust.* **925**, 1-264.
- Rodriguez, E., Jr, Weiss, D. A., Yang, J. H., Menshenina, J., Ferretti, M., Cunha, T. J., Barcellos, D., Chan, L. Y., Risbridger, G., Cunha, G. R. et al. (2011). New insights on the morphology of adult mouse penis. *Biol. Reprod.* **85**, 1216-1221.
- Rodriguez, E., Jr, Weiss, D. A., Ferretti, M., Wang, H., Menshenina, J., Risbridger, G., Handelsman, D., Cunha, G. and Baskin, L. (2012). Specific morphogenetic events in mouse external genitalia sex differentiation are responsive/dependent upon androgens and/or estrogens. *Differentiation* **84**, 269-279.
- Rortveit, G., Daltveit, A. K., Hannestad, Y. S. and Hunskaar, S; Norwegian EPINCONT Study. (2003). Urinary incontinence after vaginal delivery or cesarean section. *N. Engl. J. Med.* **348**, 900-907.
- Sasaki, C., Yamaguchi, K. and Akita, K. (2004). Spatiotemporal distribution of apoptosis during normal cloacal development in mice. *Anat. Rec. A Discov. Mol. Cell Evol. Biol.* **279A**, 761-767.
- Schlomer, B. J., Ferretti, M., Rodriguez, E., Jr, Blaschko, S., Cunha, G. and Baskin, L. (2013). Sexual differentiation in the male and female mouse from days 0 to 21: a detailed and novel morphometric description. *J. Urol.* **190**, 1610-1617.
- Seifert, A. W., Harfe, B. D. and Cohn, M. J. (2008). Cell lineage analysis demonstrates an endodermal origin of the distal urethra and perineum. *Dev. Biol.* **318**, 143-152.
- Seifert, A. W., Bouldin, C. M., Choi, K.-S., Harfe, B. D. and Cohn, M. J. (2009a). Multiphasic and tissue-specific roles of sonic hedgehog in cloacal septation and external genitalia development. *Development* **136**, 3949-3957.
- Seifert, A. W., Yamaguchi, T. and Cohn, M. J. (2009b). Functional and phylogenetic analysis shows that Fgf8 is a marker of genital induction in mammals but is not required for external genital development. *Development* **136**, 2643-2651.
- Shapiro, E., Huang, H.-Y. and Wu, X.-R. (2000). Uroplakin and androgen receptor expression in the human fetal genital tract: insights into the development of the vagina. *J. Urol.* **164**, 1048-1051.
- Shiroyanagi, Y., Liu, B., Cao, M., Agras, K., Li, J., Hsieh, M. H., Willingham, E. J. and Baskin, L. S. (2007). Urothelial sonic hedgehog signaling plays an important role in bladder smooth muscle formation. *Differentiation* **75**, 968-977.
- Suzuki, K., Adachi, Y., Numata, T., Nakada, S., Yanagita, M., Nakagata, N., Evans, S. M., Graf, D., Economides, A., Haraguchi, R. et al. (2012). Reduced BMP signaling results in hindlimb fusion with lethal pelvic/urogenital organ aplasia: a new mouse model of sirenomelia. *PLoS ONE* **7**, e43453.
- Tasian, G., Cunha, G. and Baskin, L. (2010). Smooth muscle differentiation and patterning in the urinary bladder. *Differentiation* **80**, 106-117.
- Thomson, A. A., Timms, B. G., Barton, L., Cunha, G. R. and Grace, O. C. (2002). The role of smooth muscle in regulating prostatic induction. *Development* **129**, 1905-1912.
- Timms, B. G., Mohs, T. J. and Didio, L. J. (1994). Ductal budding and branching patterns in the developing prostate. *J. Urol.* **151**, 1427-1432.
- Tomlinson, D. C., Freestone, S. H., Grace, O. C. and Thomson, A. A. (2004). Differential effects of transforming growth factor-beta1 on cellular proliferation in the developing prostate. *Endocrinology* **145**, 4292-4300.
- Viana, R., Batourina, E., Huang, H., Dressler, G. R., Kobayashi, A., Behringer, R. R., Shapiro, E., Hensle, T., Lambert, S. and Mendelsohn, C. (2007). The development of the bladder trigone, the center of the anti-reflux mechanism. *Development* **134**, 3763-3769.
- Wang, C., Gargollo, P., Guo, C., Tang, T., Mingin, G., Sun, Y. and Li, X. (2011). Six1 and Eya1 are critical regulators of peri-cloacal mesenchymal progenitors during genitourinary tract development. *Dev. Biol.* **360**, 186-194.

- Wanigasekara, Y., Kepper, M. E. and Keast, J. R.** (2003). Immunohistochemical characterisation of pelvic autonomic ganglia in male mice. *Cell Tissue Res.* **311**, 175-185.
- Weiss, D. A., Rodriguez, E., Jr, Cunha, T., Menshenina, J., Barcellos, D., Chan, L. Y., Risbridger, G., Baskin, L. and Cunha, G.** (2012). Morphology of the external genitalia of the adult male and female mice as an endpoint of sex differentiation. *Mol. Cell. Endocrinol.* **354**, 94-102.
- Wiese, C. B., Ireland, S., Fleming, N. L., Yu, J., Valerius, M. T., Georgas, K., Chiu, H. S., Brennan, J., Armstrong, J., Little, M. H. et al.** (2012). A genome-wide screen to identify transcription factors expressed in pelvic Ganglia of the lower urinary tract. *Front. Neurosci.* **6**, 130.
- Yamada, G., Satoh, Y., Baskin, L. S. and Cunha, G. R.** (2003). Cellular and molecular mechanisms of development of the external genitalia. *Differentiation* **71**, 445-460.
- Yan, H. and Keast, J. R.** (2008). Neurturin regulates postnatal differentiation of parasympathetic pelvic ganglion neurons, initial axonal projections, and maintenance of terminal fields in male urogenital organs. *J. Comp. Neurol.* **507**, 1169-1183.
- Yang, J. H., Menshenina, J., Cunha, G. R., Place, N. and Baskin, L. S.** (2010). Morphology of mouse external genitalia: implications for a role of estrogen in sexual dimorphism of the mouse genital tubercle. *J. Urol.* **184**, 1604-1609.
- Yucel, S. and Baskin, L. S.** (2004). An anatomical description of the male and female urethral sphincter complex. *J. Urol.* **171**, 1890-1897.